Carbohydrate Polymers 112 (2014) 125–133

Contents lists available at ScienceDirect

Carbohydrate Polymers

journal homepage: www.elsevier.com/locate/carbpol

True molecular solutions of natural cellulose in the binary ionic liquid-containing solvent mixtures

Dmitry M. Rein [a,*], Rafail Khalfin [a], Noemi Szekely [b], Yachin Cohen [a]

[a] Faculty of Chemical Engineering, Technion – Israel Institute of Technology, Haifa 32000, Israel
[b] Jülich Centre for Neutron Science, Forschungszentrum Jülich GmbH Outstation at MLZ, 85747 Garching, Germany

ARTICLE INFO

Article history:
Received 27 January 2014
Received in revised form 23 April 2014
Accepted 22 May 2014
Available online 2 June 2014

Keywords:
Cellulose true molecular solution
Amorphous amphiphilic cellulose
Binary solvent mixture
Small-angle neutron and X-ray diffraction

ABSTRACT

Evidence is presented for the first time of true molecular dissolution of cellulose in binary mixtures of common polar organic solvents with ionic liquid. Cryogenic transmission electron microscopy, small-angle neutron-, X-ray- and static light scattering were used to investigate the structure of cellulose solutions in mixture of dimethyl formamide and 1-ethyl-3-methylimidazolium acetate. Structural information on the dissolved chains (average molecular weight $\sim 5 \times 10^4$ g/mol; gyration radius ~36 nm, persistence length ~4.5 nm), indicate the absence of significant aggregation of the dissolved chains and the calculated value of the second virial coefficient $\sim 2.45 \times 10^{-2}$ mol ml/g^2 indicates that this solvent system is a good solvent for cellulose. More facile dissolution of cellulose could be achieved in solvent mixtures that exhibit the highest electrical conductivity. Highly concentrated cellulose solution in pure ionic liquid (27 wt.%) prepared according to novel method, utilizing the rapid evaporation of a volatile co-solvent in binary solvent mixtures at superheated conditions, shows insignificant cellulose molecular aggregation.

1. Introduction

One major disadvantage of natural cellulose, regarding its industrial application, is that due to its crystal fibril structure and the significant presence of intermolecular hydrogen bonding and hydrophobic interactions (Medronho, Romano, Miguel, Stigsson, & Lindman, 2012), it is insoluble in common solvents. Nevertheless after years of research many specific cellulose solvents were found, some of which are used now in the manufacture of commercial cellulose products (viscose and cuprammonium fibers, Lyocell®, etc.).

Derivatives of cellulose (Hunt, Newman, Scheraga, & Flory, 1956) or its metallo-complexes (Burchard & Klufers, 1994) are formed by an interaction between cellulose and the corresponding solvent components. In such solutions the macromolecules of cellulose are claimed to be completely separated from each other, and their dimension in the dissolved state is defined by its gyration radius (R_g), which is close to the size of a single macromolecule. For example, in cadmium complexing Cd-tris (2 aminoethyl) amine solution, the size of cellulose particles is equal to about 20 nm (Saalwachter et al., 2000; Schulz, Seger, & Buchard, 2000).

The fast cellulose dissolution could be realized in the alkali–urea solvents, bringing the cellulose macromolecules into the aqueous solution by forming the hydrogen-bonded complex networks. The mean size of the self-assembled solvent-cellulose clusters in these solvents is 60–160 nm (Luo & Zhang, 2013).

Dissolution of cellulose in the so-called "direct solvents" does not rely either on complex formation or derivatization of cellulose. Direct solvents transfer the polymer into solution by the mechanism of physical solvation. Relatively large dimensions of aggregates have been evaluated for cellulose dissolved in direct solvents. For example, diluted solutions of cellulose in N-methylmorpholine-N-oxide (NMMO) exhibit an R_g value of about 200 nm (Arndt, Morgenstern, & Roder, 2002; Drechsler, Radosta, & Vorwerg, 2000; Roder & Morgenstern, 1999), which considerably exceeds that of the isolated macromolecule.

Thus, it may be assumed that with alkali–urea and direct solvents the condition of a true molecular solution of cellulose is not achieved.

Ionic liquids (IL) are a unique class of direct solvents for cellulose, which have attracted significant interest due to their excellent solvation characteristics, low toxicity and volatility leading to facile recovery (Mizumo, Marwanta, Matsumi, & Ohno, 2004; Swatloski, Spear, Holbrey, & Rogers, 2002; Wang, Gurau, & Rogers, 2012).

* Corresponding author. Tel.: +972 4 8292113; fax: +972 4 829 5672.
E-mail addresses: cerycdr@tx.technion.ac.il, d_m_rein@yahoo.com (D.M. Rein), rafail@tx.technion.ac.il (R. Khalfin), n.szekely@fz-juelich.de (N. Szekely), yachinc@tx.technion.ac.il (Y. Cohen).

http://dx.doi.org/10.1016/j.carbpol.2014.05.059
0144-8617/

However, even in one of the most efficient IL solvent, 1-ethyl-3-methylimidazolium acetate (EMIMAc) (Cheng et al., 2012; Kyllonen et al., 2013; Rinaldi, 2011; Zavrel, Bross, Funke, Buchs, & Spiess, 2009) there is evidence for aggregates with R_g about 150 nm, much higher than that of a single cellulose macromolecule of the same molecular weight (Kuzmina, Sashina, Troshenkowa, & Wawro, 2010), presumably due to undissolved solvated cellulose crystals. It was shown that, according to rheological measurements, the thermodynamic properties of EMIMAc correspond to the properties of a θ solvent for cellulose (Gericke, Schlufter, Liebert, Heinze, & Budtova, 2009; Sescousse, Le, Ries, & Budtova, 2010).

In recent years it was revealed that mixtures of polar organic solvents with a small fraction of IL can instantaneously dissolve cellulose even at high concentration (Gericke, Liebert, El Seoud, & Heinze, 2011; Luo & Neogi, 2009; Rinaldi, 2011; Xu, Zhang, Zhao, & Wang, 2013). However, a reasonable explanation of this effect is still lacking. According to one explanation, solvation effects such as the chemical interactions due to the specific composition of the solute and solvent play a major role. These can be due to acid–base or polar interactions, or an ability to form cyclic arrangements of solvent and cellulose during dissolution (Remsing, Liu, Sergeyev, & Moyna, 2008; Pinkert, Marsh, & Pang, 2010). According to another explanation, the enhanced cellulose dissolution in co-solvent/IL mixtures is caused by the increased concentration of the "free" anions from the dissociated IL owing to the preferential solvation of the cations by the aprotic polar solvents (Xu et al., 2013). A third explanation considers possible electric interactions between cellulose chains, which are sufficiently weakened in the co-solvent/IL environment with high relative dielectric permittivity (the dielectric constant for the imidazolium-based IL it is about 10, Wakai, Oleinikova, Ott, & Weingartner, 2005) (Stana-Kleinschek & Ribitsch, 1998). It was noted that, based on rheological measurements, EMIMAc/dimethyl sulfoxide mixture is more like a θ solvent for cellulose, and the thermodynamic properties of EMIMAc/dimethyl sulfoxide mixtures are similar with those of ILs. The conformation of cellulose in ILs would not be changed with the addition of dimethyl sulfoxide not only in the dilute cellulose concentrations, but also in the entanglement concentrations (Lv et al., 2012).

The decisive influence of the cellulose amphiphilicity and hydrophobic interactions on the processes of its dissolving currently is being actively discussed in scientific literatures (Glasser et al., 2012; Medronho et al., 2012). In previous studies we described a novel phenomenon: outstanding amphiphilic properties inherent to cellulose molecules dissolved in co-solvent/IL binary mixtures and to cellulose in the amorphous state in hydrogels regenerated from these solutions, as evident in their ability to form a stabilizing coating for oil-in-water (O/W) and water-in-oil (W/O) emulsions (Rein, Khalfin, & Cohen, 2012). Similar properties were also found in cellulose regenerated from the phosphoric acid (Jia et al., 2013). We had presented the hypothesis that this manifestation of cellulose's amphiphilic character is made possible by its molecular dissolution in the solvent mixture prior to the emulsification process (Rein et al., 2012). The amorphous cellulose hydrogel, received on the basis of these free-molecular-chain solutions, also holds noticeable chain mobility and pronounced amphiphilic properties (Rein et al., 2012), which is consistent with the previously detected phenomena that even in the crystalline state, in disordered structural regions, plasticized by sorbed water, there is evidence for the increased mobility of cellulose chain segments. (Bradley & Carr, 1976; Froix & Nelson, 1975), a thorough analysis of the molecular state of cellulose in solution in ionic liquids and their binary solvent mixtures using light scattering and transmission electron microscopy methods is lacking. For this purpose we seek to utilize a combination of scattering techniques, static light scattering (SLS), small-angle X-ray and neutron scattering (SAXS and SANS) with cryogenic transmission electron microscopy (cryo-TEM).

2. Materials and methods

Microcrystalline cellulose powder Avicel® with nominal molecular weight (given by the supplier) $\sim 4.6 \times 10^4$ g/mol (degree of polymerization 295 and particle size in the range of 20–160 μm), and ionic liquid EMIMAc of 90% purity, were obtained from Sigma–Aldrich. EMIMAc and cellulose were dried in a vacuum oven at 60 °C and 0.26 kPa for at least 24 h. Chloroform, dichloromethane (DCM), dimethyl formamide (DMF), deuterated DMF (DMF-d_7), acetonitrile and propylene carbonate were purchased from Sigma–Aldrich. These chemicals were used without additional purification. Unless otherwise stated, the weight percentages of the components were calculated based on the total composition of the final mixture.

2.1. Dissolution of cellulose

Dissolution of cellulose was realized in two stages so as to reduce the aggregation (Rein et al., 2012; Rinaldi, 2011). First, cellulose was dispersed in a specific volume of the co-solvent. Next, the required volume of EMIMAc was added into the suspension, and the mixture was heated to 90 °C using magnetic stirring during about 10 min. Subsequently, the obtained solution was cooled to room temperature and was not further treated.

2.2. Equipment and characterization methods

The morphology of the solutions was investigated by cryogenic transmission electron microscope (cryo-TEM) T12G2 (FEI Co., Netherlands). Vitrified samples for cryo-TEM (Talmon, 1996) were prepared in a controlled environment vitrification system (CEVS) (Bellare, Davis, Scriven, & Talmon, 1988).

SLS measurements were carried out with a goniometer BI-200SM (Brookhaven Instruments Corp., USA) using an argon-ion laser (wavelength 514.5 nm). Data obtained at several concentrations (0.4–4 wt.%) and scattering angles (30–150°) were evaluated by the common Zimm plot yielding the root-mean-square R_g, weight-average molar mass M_w and the second osmotic virial coefficient A_2 (Debye, 1944; Zimm, 1945). The indices of the solvent refraction n_o ($n_o = 1.44$ for the investigated DMF/EMIMAc mixture with molar ratio 9:1) and the mass concentration (c) increment of the solution refraction index dn/dc (for investigated DMF/EMIMAc mixture $dn/dc = 0.061 \pm 0.06\ cm^3/g$) were measured by a differential refractometer BI-DNDC (Brookhaven Instruments Corp., USA).

Electrical conductivity of solvent mixtures was measured with a Precision Impedance Analyzer Agilent 4294A (Agilent Technologies) at 0.5 V and 10 kHz. Each sample was analyzed in triplicate and the mean values were plotted (average measurements error about 12%).

X-ray diffractometry of the samples was performed using a small/wide-angle diffractometer (Molecular Metrology SAXS/WAXS system) equipped with a sealed microfocus tube (MicroMax-002+S) emitting CuK_α radiation, two Göbel mirrors, three-pinhole slits, and generator that is powered at 45 kV and 0.9 mA. The scattering patterns were recorded by a two-dimensional position sensitive wire detector positioned 150 cm behind the sample. The solutions were sealed in thin-walled glass capillaries about 2 mm in diameter and 0.01 mm wall thickness, and measured under vacuum at the ambient temperature. The scattered intensity $I(q)$ was recorded at the interval $0.07 < q < 2.7\ nm^{-1}$, where q is the scattering vector $q = 4\sin(\theta)/\lambda$, 2θ is the scattering angle and λ is the incident wavelength. The scattering intensity was normalized with respect to time, solid-angle, primary beam

Table 1
Main electrical and dissolution properties of investigated co-solvents.

Co-solvent	Dielectric constant[a]	Dipole moment[a], *D*	Electrical conductivity (mS/cm)	MDA
Chloroform	4.7	1.04	0.02	1:1
DCM	9.1	1.63	0.005	5:1
DMF	36.7	3.82	0.03	10:1
Acetonitrile	37.5	3.92	0.07	1:1
Propylene carbonate	65.3	4.92	0.04	3:1

[a] At 20 °C, according to Dickinson and Covington (1973), 1 D = 3.33564×10^{-30} C m. For comparison, dielectric constant of pure EMIMAc: 10 (Wakai et al., 2005), electrical conductivity – 3.5 mS/cm.

intensity, capillary diameter, transmission, and the Thompson factor. Scattering of the solvents, empty capillary and electronic noise were subtracted.

Small angle neutron scattering (SANS) experiments were conducted on the KWS2 beamline (Jülich Center for Neutron Science) at the FRM-II reactor (Maier-Leibnitz Zentrum, TU Münich). λ was 0.48 nm, and an aperture of 8 mm × 8 mm was used. The experiments were carried out at sample to detector distances of 4, 8 and 20 m and the measurable scattering vector range was $0.02 < q < 0.8\ nm^{-1}$. The samples were studied in quartz cuvettes (2 mm pathlength) at 20 °C. The data were reduced to absolute units (cm^{-1}) and background scattering from the pure polymer solutions was subtracted, as reported previously (Granite, Radulescu, Pyckhout-Hintzen, & Cohen, 2011). To provide contrast with the hydrogen containing cellulose and EMIMAc, the 4 wt.% solution of natural cellulose in binary solvent mixture of deuterated DMF-d_7/EMIMAc (molar ration 9:1) was used for SANS measurements.

3. Results and discussion

The ability of polar aprotic co-solvents/EMIMAc mixtures for enhanced cellulose dissolution is of high practical interest (Gericke et al., 2011; Luo & Neogi, 2009; Rinaldi, 2011; Xu et al., 2013). For comparison of the dissolution ability of various solvent mixtures, we define the term "mixture dissolution ability (MDA)". This is a measure of the highest molar ratio of co-solvent to IL in which an apparent "instantaneous dissolution" of cellulose still occurs, as evaluated in obtaining a transparent homogeneous solution of 4 wt.% cellulose at 90 °C by not more than 5 min of intensive mixing followed by cooling of the solution to room temperature without losing its visual transparency. At this temperature and concentration cellulose dissolution was found to be most sensitive to solvent composition, as shown in the Supplementary information. Fig. 1 presents pictures of cellulose, dissolved in EMIMAc with different co-solvents at their MDA conditions, as listed in Table 1. For the DMF/EMIMAc solvent mixtures, separate pictures exhibit a 2 wt.% cellulose solution at solvent molar ratio 11:1 (Fig. 1f), compared to a picture of a 2 wt.% solution at a slightly higher molar ratio (12:1), which is significantly more turbid (Fig. 1g). Table 1 also lists characteristic electrical properties of these common co-solvents. As evident from the data presented in Table 1, DMF and, to some extent DCM, have higher MDA then the other polar co-solvents studied: a fact that cannot be explained on the basis of any electrical characteristic we have considered.

3.1. Electrical conductivity of co-solvent/IL mixtures and cellulose solutions

As was mentioned above, the enhanced cellulose dissolution in IL containing solvents has been related to the increased free anion concentration and its interaction with cellulose, in particular the methyl hydroxyl groups. In the mixed system of IL with polar solvents, this effect may be enhanced by shifting the IL dissociation equilibrium due to preferential solvation of its cations by the co-solvent. Rise of the free ion mobility, at increased temperature and reduced viscosity with increasing co-solvent concentration also contribute to this effect. The cellulose solution concentration may also influence its dissolution due to its effect on the interaction and mobility characteristics. Such variation in the concentration and mobility of free ions should inevitably influence the electrical conductivity of the solvent mixture and cellulose solution. It is therefore of interest to relate the solvent mixture's and cellulose solution's electrical conductivity with their cellulose dissolution ability. Fig. 2 displays the influence of solvent composition and temperature on the electrical conductivity of pure DMF/EMIMAc mixtures and cellulose solutions at moderate concentrations (less than 6 wt.%) in these solvent mixtures. It can be seen that at all the investigated temperatures the solvent mixture and cellulose solution electrical conductivity initially increases with increasing co-solvent/IL molar ratio, with subsequent decrease in electrical conductivity at highly diluted EMIMAc solutions. It is necessary to note that the conductivity of cellulose solutions follows the conductivity of pure solvent mixture. The electrical conductivity maximum for all the studied co-solvents and temperatures are in the common range of co-solvent/EMIMAc molar ratio of 1:1–2:1. Similar dependence of electrical conductivity on dilution and temperature of organic co-solvent/IL and water/IL mixtures is well known (Hardelin et al., 2012; Koddermann et al., 2012; Rein et al., 2012; Vila, Gines, Pico, et al., 2006; Vila, Gines, Rilo, Cabeza, & Varela, 2006).

The results presented in Fig. 2 indicate that the dissolved cellulose at moderate concentrations practically has no effect on the

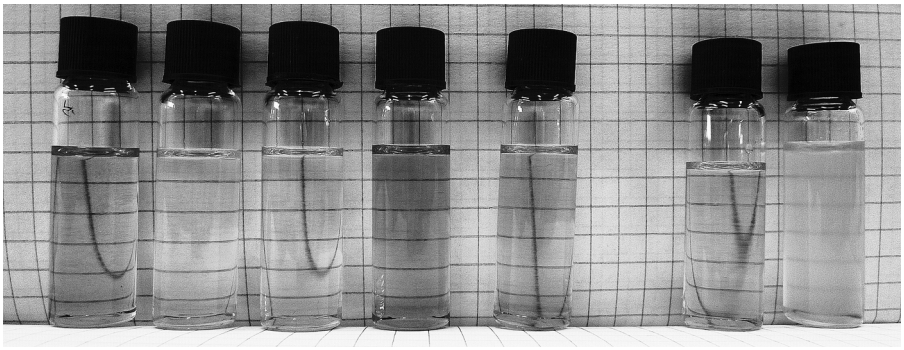

Fig. 1. 4 wt.% cellulose solutions in the different co-solvent/EMIMAc mixtures at their MDA conditions (according to Table 1): (a) chloroform, (b) DCM, (c) DMF, (d) acetonitrile; (e) propylene carbonate. For comparison only, not corresponding to MDA conditions: 2 wt.% cellulose solutions in DMF/EMIMAc mixture with molar ratio: (f) 11:1; (g) 12:1 (note that this solution was transparent at 90 °C). All solutions were photographed at room temperature.

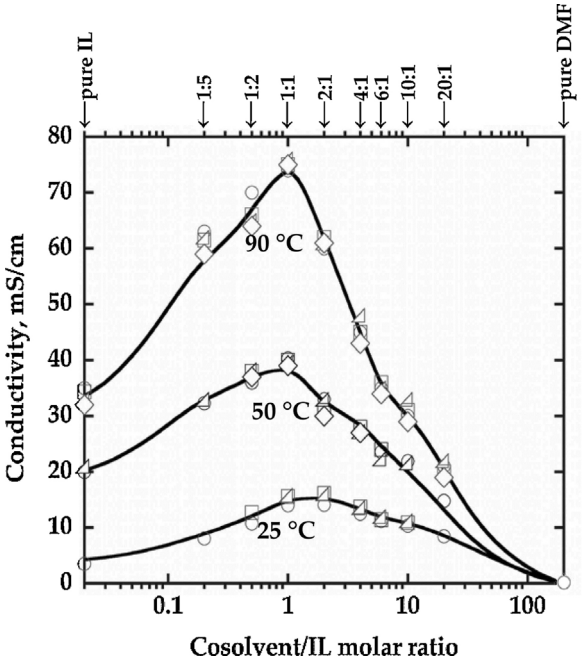

Fig. 2. Influence of DMF/EMIMAc molar ratio, cellulose concentration (◯ – 0% (pure DMF/EMIMAc mixture); ◿ – 0.1 wt.%; □ – 2 wt.%; ◊ – 6 wt.%) and solution temperature (shown near lines) on its electrical conductivity.

solution's electrical conductivity, while the temperature and co-solvent/IL ratio are significant.

However, as cellulose concentration is increased above about 6 wt.% its effect on electrical conductivity becomes noticeable. This influence is more pronounced at increased temperatures, particularly at 90 °C, as shown in Fig. 3. In addition to the lower ion mobility at these conditions, it may also reflect the effect of possible supramolecular structures of cellulose in solution, as has been suggested (Song, Niu, Wang, & Zhang, 2011). It should be noted, in particular, that our experiments have shown that at higher cellulose

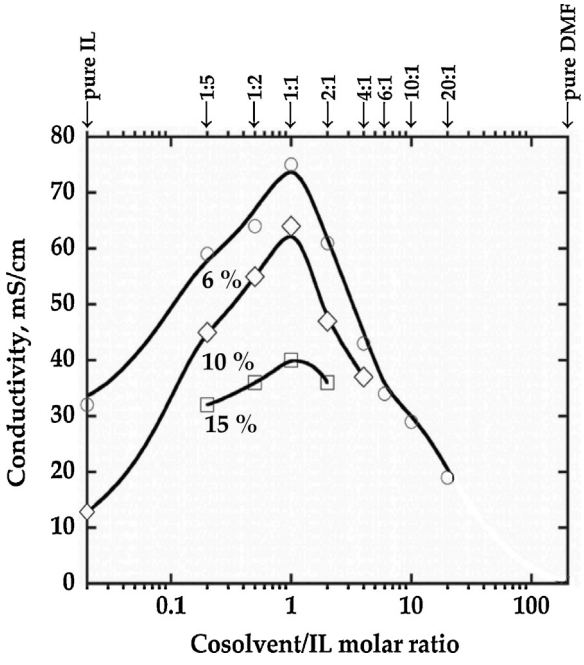

Fig. 3. Influence of DMF/EMIMAc molar ratio and solution concentration (shown near lines) on its electrical conductivity at 90 °C.

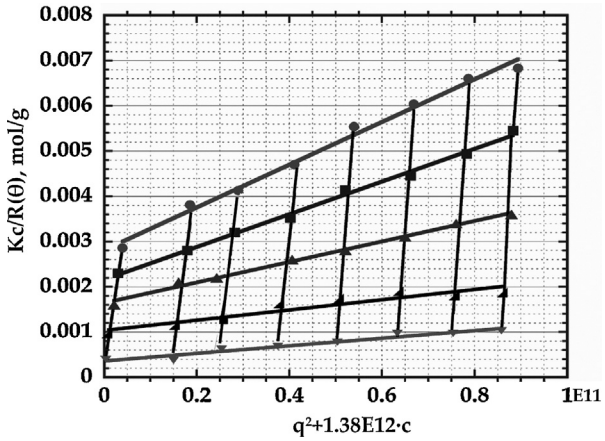

Fig. 4. Zimm plot of cellulose solutions (obtained by diluting a stock 4 wt.% solution) in binary solvent mixture DMF/EMIMAc (molar ratio 9:1) at 20 °C.

concentrations, above 5 wt.%, more facile dissolution of cellulose (visually almost instantaneous) is achieved at the co-solvent/IL ratio that exhibits the highest electrical conductivity.

3.2. Cellulose aggregates size in solution

The clear appearance of cellulose solutions in binary co-solvent/IL mixtures is a necessary but not sufficient condition of cellulose dissolution at the molecular level. It is thus important to probe the state of the dissolved cellulose chains. SLS measurements of cellulose solutions in DMF/EMIMAc (molar ratio 9:1) are presented in Fig. 4 as a Zimm plot. Its analysis yields M_w about $(5 \pm 1) \times 10^4$ g/mol, which is in good accord with the nominal M_w given by the supplier (4.6×10^4 g/mol), R_g of 36 ± 8 nm and a value $A_2 = (2.45 \pm 0.22) \times 10^{-2}$ mol ml/g^2. This Zimm analysis attests the molecular dissolution of cellulose by our method; SLS also confirms that the solvent mixture used is indeed a good solvent for cellulose. Analysis of scientific publications proves that in many modern direct solvents cellulose dissolves in the form of molecular aggregates ($R_g \gg 30$ nm), but not real molecular solutions (Arndt et al., 2002; Kuzmina et al., 2010). In solvents, in which cellulose could be dissolved in the form of a real molecular solution (Drechsler et al., 2000; McCormick, Callais, & Hutchinson, 1985) the coefficient A_2 is usually about 10^{-4}–10^{-3} mol ml/g^2, which is one order of magnitude lower, than we found in our investigation. On the other hand, according to Trap and Hermans (1954) reported a value of $A_2 = 2.5 \times 10^{-2}$ mol ml/g^2 for the real molecular solution of carboxymethylcellulose in aqueous solution of NaCl at concentration of about 0.01 mol/l (which contains a large amount of mobile ions in a low-viscosity environment similar to the solvent mixture investigated by us).

3.3. Small angle neutron and X-ray diffraction

A further probe of the molecular state of the dissolved cellulose chains is provided by small angle scattering measurements of X-rays and neutrons (SAXS, SANS). Fig. 5a presents SANS data from 4 wt.% cellulose in DMF-d_7/EMIMAc (molar ratio 9:1), with that of the solvent mixture alone. The lack of significant excess scattering at low angles is a strong indication for the lack of significant aggregation of cellulose chains in this solvent mixture, even at rather low IL content, in accordance with the SLS measurements. After subtraction of the solvent scattering the data can be fit by the Ornstein–Zernike equation, as applied to a semidilute polymer solution (Daoud et al., 1973), which is given as

$$I(q) = \frac{I(0)}{1 + q^2\xi^2} \quad (1)$$

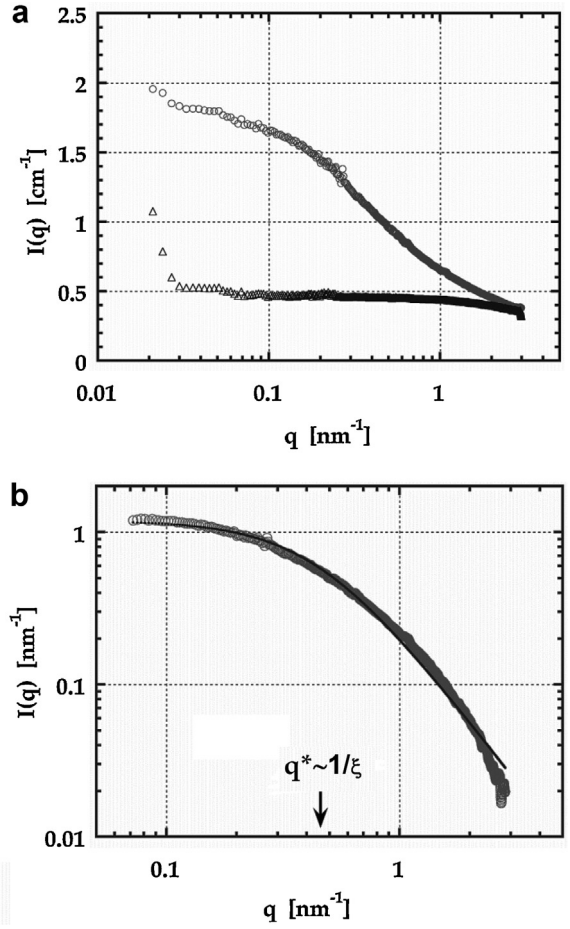

Fig. 5. SANS patterns from 4 wt.% cellulose solution in DMF-d_7/EMIMAc (9:1 molar ratio) – open circles: (a) before background subtraction, with the scattering from the solvent mixture (triangles) and (b) after background subtraction, with a fit of Eq. (1) – solid line.

for which: $I(0) = \Delta\rho^2\varphi^2/K_{os}$, where φ is the polymer volume fraction, $\Delta\rho = (\rho_p - \rho_s)$ is the difference in scattering length density (SANS) or electron density (SAXS) between polymer and solvent (ρ_p, ρ_s, respectively), ξ is the correlation length beyond which the inter-segmental excluded volume interactions are screened by the chain overlap, and $K_{os} = (c/RT)(d\pi/dc)$ is the osmotic modulus, where R, T are the gas constant and absolute temperature, π is the osmotic pressure and c is the polymer concentration. Application of Eq. (1) is valid at polymer concentration beyond that of chain overlap ($c > c* = M/2^{3/2}N_{AV}R_G^3$), and at small angles, where $q\xi < 1$ (Cloizeaux & Jannink, 1990). Fitting Eq. (1) to the data in Fig. 5a, after subtraction of the background solvent scattering, as shown in Fig. 5b, yields an estimation of the correlation length $\xi = 2.3$ nm, for which the suitable fitting range is $q < q^*$ as indicated in Fig. 5b. An overlap concentration about 0.008 g/cm^3 can be estimated as mentioned above using the values of M and R_G measured by SLS, a concentration that is nearly fivefold lower than that of the studied solution (4 wt.%: $c \sim 0.039$ g/cm^3). The estimated correlation length happens to be close to that measured for polystyrene ($M_w \sim 1.1 \times 10^5$) in toluene at similar concentration and is in accord with the predicted value of ξ/R_G at the same reduced concentration (c/c^*) (Hamada, Kinugasa, Hayashi, & Nakajima, 1984) (note a factor of $2^{3/2}$ difference in the definition of c^*), following a relation which has been theorized to have universal attribute. (Hailer & Cannell, 1983) Thus SANS measurements present a clear indication for true molecular dissolution of cellulose at 4wt.% in the solvent mixture of DMF/EMIMAc (9:1 molar ratio).

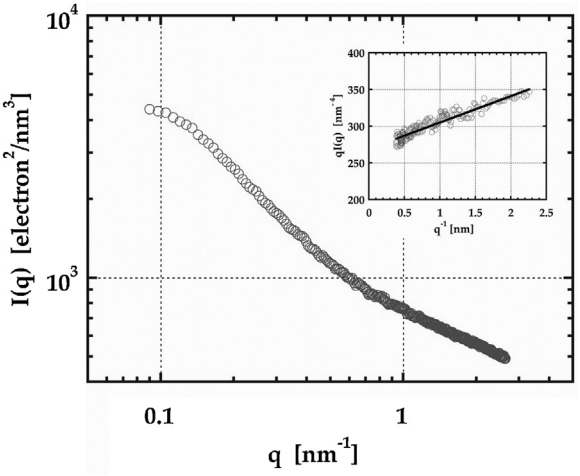

Fig. 6. SAXS patterns from 0.4 wt.% cellulose solution in DMF/EMIMAc (9:1 molar ratio), before background subtraction. Inset: linear fit of Eq. (2).

Dissolved cellulose chains have been considered to be semiflexible polymers, and the persistence length of cellulose and several of its derivatives, in a number of solvents, has been reported based on viscosity measurements to be in a range about 4–20 nm, depending on derivatization and solvent (Kamide & Saito, 1983). It is thus of interest to compare these values with the persistent length determined for underivatized cellulose dissolved in the DMF/EMIMAc (9:1 molar ratio) solvent mixture. This is approached by SAXS measurements rather than SANS, as they provide better signal above background at large q since the effect of concentration fluctuations is less prominent due to the smaller contrast between the two solvent components. Fig. 6 exhibits the SAXS pattern from the 0.4 wt.% cellulose solution in DMF/EMIMAc (9:1 molar ratio). The value of the persistence length can be evaluated by the empirical relation based on computer simulations of semiflexible chains, given as (Hsu, Paul, & Binder, 2012)

$$qI(q) = \frac{A}{L}\left(\pi + \frac{1.9}{qL_P}\right) \quad (2)$$

where A is a constant, and L_p and L are the persistence and contour lengths, respectively. The inset in Fig. 6 shows a plot of Eq. (2) evaluated from the SAXS data, yielding a value $L_p \sim 4.5$ nm for the persistence length from the linear fit in the region of validity $q > 2/L_p \sim 0.44$ nm^{-1}. This value is close to the estimated lower limit of persistent lengths estimated for cellulose derivatives (such as cellulose acetate) in organic solvents (Kamide & Saito, 1983) and significantly lower than the value for cellulose dissolved in some unique solvents such as cadmium ethylenediamine hydroxide or iron sodium tartrate (Kamide & Saito, 1983) or N,N-dimethyl acetamide/lithium chloride (McCormick et al., 1985). This again may be a manifestation of cellulose true molecular dissolution.

3.4. Novel method for preparation of highly concentrated cellulose solutions

There is particular interest in obtaining highly concentrated cellulose solutions in ILs, which can be used for a fabrication of novel osmosis membranes (Li, Zhu, Zhu, & Xu, 2011) and inexpensive, eco-compatible proton conduction medium for electric storage devices (Johari, Kudin, Ali, Winie, & Yahya, 2009). According to the published literature, preparation of highly concentrated cellulose solutions in ILs demands long mixing time on the order of tens of hours (Gericke et al., 2009; Song et al., 2011; Swatloski et al., 2002). We suggest a novel method for fabrication of highly concentrated solutions of cellulose in pure IL utilizing the rapid

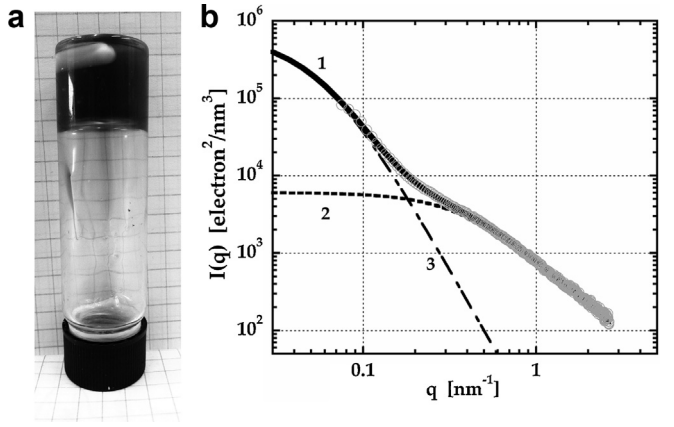

Fig. 7. Highly viscous 27 wt.% cellulose solution in pure EMIMAc obtained by rapid evaporation of DCM from EMIMAc mixture (a); SAXS pattern of this solution (open circles) (b): full fitting according to Eq. (4) (line 1); fitting of high-q pattern part by Eq. (1) (line 2) and low-q part by Eq. (3) (line 3).

evaporation of a volatile component of co-solvent/IL mixture at superheated conditions in a specifically designed pressure vessel. Fast cellulose dissolution in the mixed solvent is realized at conditions of vapor saturation equilibrium at the elevated temperature and pressure. Subsequent controlled release of pressure at the elevated temperature causes rapid evaporation of the volatile co-solvent leaving behind a concentrated cellulose/IL solution. Any residual co-solvent may be removed under vacuum from the thin film of concentrated cellulose solution. The entire process takes only a few minutes, instead of hours. Fig. 7a exhibits a very viscous concentrated solution of cellulose in pure EMIMAc (27 wt.%), obtained by evaporating the volatile co-solvent DCM at superheated conditions (initial cellulose concentration 13 wt.% in the original solvent mixture DCM/EMIMAc = 3:1, which possesses a suitable viscosity (about 0.1 Pa s), allowing uniform cellulose dispersion at room temperature and its dissolution under DCM vapor saturation equilibrium pressure 0.73 MPa at temperature 100 °C during about 10 min; the following DCM evaporation was realized at 0.1 MPa at the same temperature during 20 min).

We performed SAXS measurements in order to assess the state of molecular aggregation in the concentrated cellulose/EMIMAc solutions (27 wt.%), as shown in Fig. 7b. The observed pattern, viewed in double logarithmic format, exhibits a broad shoulder at intermediate values of the scattering vector q, with noticeable excess scattering at low q. This is reminiscent of the patterns that often appear in concentrated polymer solutions, sometimes termed the Picot–Benoit effect (Benoit & Picot, 1966), in which the shoulder is considered to be due to the fluctuation scattering of the dissolved chains, hence having the Lorentzian form of the Ornstein–Zernike equation (Eq. (1)). The excess low-angle scattering has been considered to be due to molecular aggregates, either permanent or dynamic. Scattering from irregular agglomerates can be modeled by the Debye–Bueche equation of an inhomogeneous material (Debye & Bueche, 1949):

$$I(q) = \frac{I_i(0)}{(1+q^2\xi_i^2)^2} \tag{3}$$

for which: $I_i(0) = 8\pi\Delta\rho^2\varphi_i^2\xi_i^3$, where φ_i and ξ_i are the volume fraction and characteristic dimension of the inhomogeneities, respectively. A combination of Eqs. (1) and (3) has been used to analyze the scattering pattern of an inhomogeneous polymer gel, which is envisioned to be composed mostly of a fluctuating semi-dilute polymer solution-like structure with embedded compact polymer inhomogeneities (Hecht, Horkay, Schleger, & Geissler, 2002):

$$I(q) = \frac{I(0)}{(1+q^2\xi^2)} + \frac{I_i(0)}{(1+q^2\xi_i^2)^2} + B \tag{4}$$

where B represents the background due to incoherent and solvent scattering. The fit of Eq. (4) to the SAXS pattern from the 27 wt.% cellulose solution in EMIMAc is shown by the solid line (1) in Fig. 7b. The fit yields the parameters given in Table 2.

Table 2
Fitted parameters of Eq. (4).

Parameter	Fitted value
ξ (nm)	2.6
$I(0)$ (electron^2/nm^3)	6000
ξ_i (nm)	18
$I_i(0)$ (electron^2/nm^3)	645 000
B (electron^2/nm^3)	430

The estimated value of the correlation length in the solution scattering function, ξ = 2.6 nm, is slightly larger than that evaluated by SANS from the 4% cellulose in DMF/EMIMAc system, 2.3 nm. This is a surprising result since ξ should decrease with polymer concentration, which in this case is widely different. Preliminary results from an ongoing study indicates a weak dependence of the correlation length on polymer concentration, contrary to the expected power law relations exhibited by semi-dilute polymer solutions, $\xi \sim \varphi^{-\alpha}$, with an exponent α being about 0.75 or 1 for good or theta solvent conditions, respectively (Cloizeaux & Jannink, 1990). According to our measurements exponent α is about 1/3. A more detailed study on this issue is currently under way.

The extent to which cellulose chains are aggregated can be estimated from the scattering pattern of Fig. 7b. The integrated intensity of a random two-phase structure with sharp interfaces, Q, is related to the volume fraction of inhomogeneities, as given by the Porod integral (Porod, 1982):

$$Q = \int_o^\infty q^2 I(q)\,dq = 2\pi^2(\rho_i - \rho_s)^2\varphi_i(1-\varphi_i) \simeq 2\pi^2(\rho_i - \rho_s)^2\varphi_i$$
$$\text{for} \quad \varphi_i \ll 1 \tag{5}$$

where φ_i and ρ_i are the volume fraction and electron density (SAXS) or scattering length density (SANS) of the inhomogeneity, respectively. Direct evaluation of φ_i by Eq. (5) requires an assumption of the aggregate density ρ_i, and calibration of absolute intensity. Alternatively, the ratio of the Porod integral of the inhomogeneity part (the low angle scattering fitted by Eq. (3)) to that of the total scattering pattern, calculated by Eq. (5) over the measured q-range only, can be taken as an indication of the fraction of the total dissolved cellulose that is contained within the aggregates. This ratio, evaluated as 0.043, confirms that the volume fraction of aggregates in solution is about 0.9%. This analysis of the SAXS measurement can be interpreted as indicating that although significant excess scattering is observed at low angles, only a small fraction of the dissolved cellulose chains are aggregated in the EMIMAc solution. The most reasonable explanation of this fact is that the evaporation process is accompanied by such a rapid increase in solution viscosity that it does not leave time for significant aggregation of the free cellulose molecules.

3.5. Cryogenic transmission electron microscopy

As mentioned above, small-angle scattering measurements indicate molecular dissolution of the cellulose chains with no apparent aggregation in suitable co-solvent/IL mixtures. As the co-solvent ration is increased, the turbid appearance of the solutions,

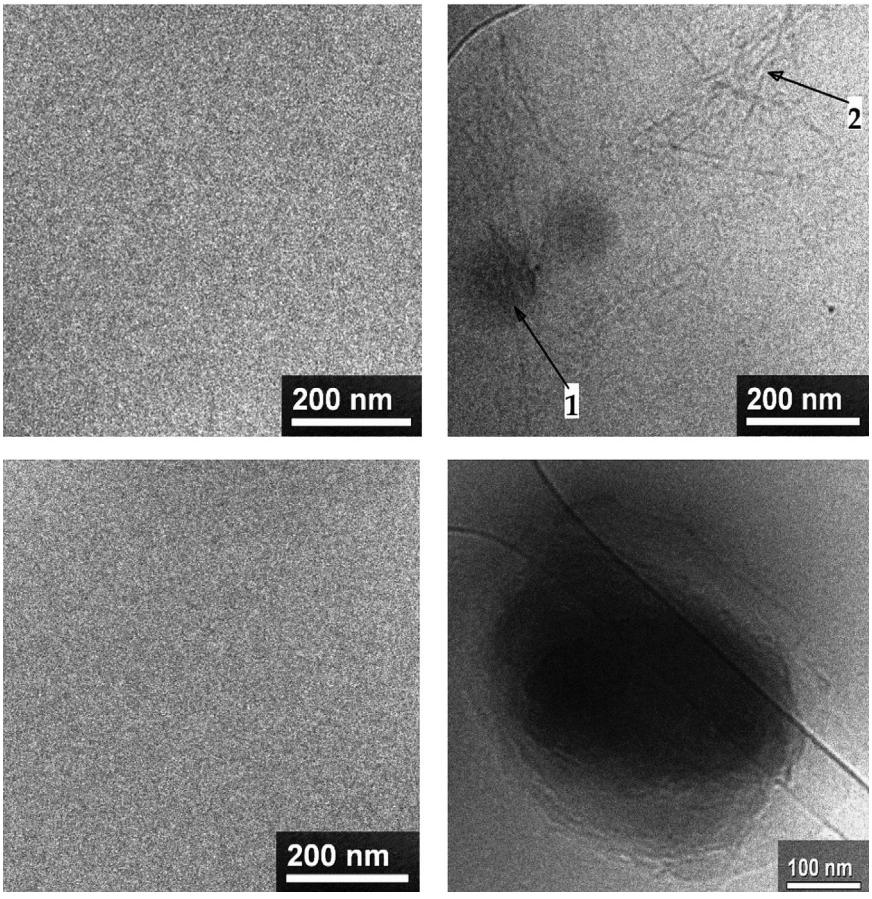

Fig. 8. Cryo-TEM images of 2 wt.% cellulose solutions in DMF/EMIMAc mixture: (a) with molar ratio 9:1; (b) turbid solution at a higher molar ratio 12:1 (1 – amorphous globule, 2 – cellulose fibril); (c) 2 wt.% cellulose solution in pure EMIMAc, obtained by full evaporating of DCM co-solvent (primary DCM/EMIMAc molar ratio 1:2, initial cellulose concentration 1.6 wt.%); (d) 2 wt.% solution of cellulose, dissolved directly in pure EMIMAc without co-solvent.

as shown in Fig. 1g, indicates the presence of aggregates. Cryo-TEM imaging is therefore useful to probe this effect by direct imaging of vitrified solutions. The lack of cellulose molecular aggregates in cryo-TEM images of DMF/EMIMAc cellulose solutions, such as that of a 2% solution in 9:1 molar ratio mixture, shown in Fig. 8a, confirms this statement. Moreover, this molecular dissolution condition remains after full evaporation of the volatile co-solvent, as shown in Fig. 8c for a 2% cellulose solution in pure EMIMAc obtained by evaporation of DCM from an original solution in DCM/EMIMAc mixture with molar ratio 1:2. Cryo-TEM images from turbid solutions, such as that shown in Fig. 8b for a 2% cellulose solution in DMF/EMIMAc at 12:1 molar ratio, clearly indicate the presence of aggregates. Aggregates are also apparent when cellulose is directly dissolved in pure EMIMAc (Fig. 8d). The cryo-TEM images indicate that cellulose aggregates in the solution containing co-solvent have a different morphology than those in the pure IL. In the first case the aggregates seem to occur in two structures: amorphous globular (Fig. 8b (1)) and fibril-like (Fig. 8b (2)). In the second case the aggregates appear as incompletely dissolved microcrystallites. It may be that in the former case, aggregates were formed when the surplus of co-solvent was added to a true solution, whereas in the latter case the aggregates are the relicts of an initial, microcrystalline cellulose structure.

4. Conclusion

We have shown, for the first time, that natural cellulose is dissolved molecularly in solvent mixtures containing common polar organic solvents ("co-solvents": chloroform, DCM, DMF, acetonitrile and propylene carbonate) with ionic liquid (1-ethyl-3-methylimidazolium acetate) at co-solvent/IL molar ratios up to 10:1. This was verified by SLS and SANS measurements which showed no evidence for molecular aggregation. Therefore, the specific parameters of cellulose chains dissolved in DCM/EMIMAc, such as molecular weight, gyration radius and second virial coefficient, could be determined by light scattering measurements from dilute solutions, a correlation length of inter-chain interactions in a semi-dilute solution could be determined by neutron scattering and the persistence length from X-ray scattering measurements. We found that more facile (visually almost instantaneous) dissolution of cellulose could be achieved in solvent mixtures that exhibit the highest electrical conductivity. We have suggested a novel method for fabrication of highly concentrated cellulose solutions in pure IL, prepared by evaporation of volatile co-solvent in binary co-solvent/IL mixture, which showed insignificant cellulose molecular aggregation.

Acknowledgments

D.M. Rein's and R. Khalfin's work was supported by a joint grant from the Center for Adsorption in Science of the Ministry of Immigrant Absorption and the Committee for Planning and Budgeting of the Council for Higher Education under the framework of the KAMEA program. This project is funded by the Israel Science Foundation Grant No. 165/11. Electron microscopy was performed at the Technion Soft Matter EM Laboratory,

supported by the Russell Berrie Nanotechnology Institute (RBNI). SANS measurements were supported by the European Commission 7th Framework Program Key Action: Strengthening the European Research Area, Research Infrastructures. Contract no.: 283883 (NMI3-II). The authors acknowledge valuable contributions and collaboration with Dr. E. Kesselman and Dr. S. Prilutzky.

Appendix A. Supplementary data

Supplementary data associated with this article can be found, in the online version, at http://dx.doi.org/10.1016/j.carbpol.2014.05.059.

References

Arndt, K.-F., Morgenstern, B., & Roder, T. (2002). Scattering function of non-substituted cellulose dissolved in N-methylmorpholine-N-oxide-monohydrate. *Macromolecular Symposia*, *162*, 109–119.

Bellare, J. R., Davis, H. T., Scriven, L. E., & Talmon, Y. (1988). Controlled environment vitrification system: An improved sample preparation technique. *Journal of Electron Microscopy Technique*, *10*, 87–111.

Benoit, H., & Picot, C. (1966). Light-scattering study of moderately concentrated macromolecular solutions. *Pure and Applied Chemistry*, *12*, 545–561.

Bradley, S. A., & Carr, S. H. (1976). Mechanical loss processes in polysaccharides. *Journal of Polymer Science: Polymer Physics Edition*, *14*, 111–124.

Burchard, W., & Klufers, P. (1994). Cellulose in Schweizers Reagens: ein stabiler, polymerer Metallkomplex hoher Kettensteifhei. *Angewandte Chemie*, *106*, 936–939.

Cheng, G., Varanasi, P., Arora, R., Stavila, V., Simmons, B. A., Kent, M. S., et al. (2012). Impact of ionic liquid pretreatment conditions on cellulose crystalline structure using 1 ethyl-3-methylimidazolium acetate. *Journal of Physical Chemistry B*, *116*, 10049–10054.

des Cloizeaux, J., & Jannink, G. (1990). *Polymers in solutions*. Oxford: Clarendon Press.

Daoud, M., Cotton, J. P., Farnoux, B., Jannink, G., Sarma, G., Benoit, H., et al. (1973). Solutions of flexible polymers: Neutron experiments and interpretation. *Macromolecules*, *8*, 804–818.

Debye, P. J. (1944). Light scattering in solutions. *Journal of Applied Physics*, *15*, 338–342.

Debye, P. J., & Bueche, A. M. (1949). Scattering by an inhomogeneous solid. *Journal of Applied Physics*, *20*, 518–525.

Dickinson, A. K., & Covington, T. (Eds.). (1973). *Physical chemistry of organic solvent systems*. London, New York: Plenum Press.

Drechsler, U., Radosta, S., & Vorwerg, W. (2000). Characterization of cellulose in solvent mixtures with N-methylmorpholine-N-oxide by static light scattering. *Macromolecular Chemistry and Physics*, *201*, 2023–2030.

Froix, M. F., & Nelson, R. (1975). The interaction of water with cellulose from nuclear magnetic resonance relaxation times. *Macromolecules*, *8*, 726–730.

Gericke, M., Schlufter, K., Liebert, T., Heinze, T., & Budtova, T. (2009). Rheological properties of cellulose/ionic liquid solutions: From dilute to concentrated states. *Biomacromolecules*, *10*, 1188–1194.

Gericke, M., Liebert, T., El Seoud, O. A., & Heinze, T. (2011). Tailored media for homoheneous cellulose chemistry: Ionic liquid/co-solvent mixtures. *Macromolecular Materials and Engineering*, *296*, 483–493.

Glasser, W. G., Atalla, R. H., Blackwell, J., Brown, R. M., Jr., Burchard, W., French, A. D., et al. (2012). About the structure of cellulose: Debating the Lindman hypothesis. *Cellulose*, *19*, 589–598.

Granite, M., Radulescu, A., Pyckhout-Hintzen, W., & Cohen, Y. (2011). Interactions between block copolymers and single-walled carbon nanotubes in aqueous solution: A small-angle neutron scattering study. *Langmuir*, *27*, 751–759.

Hailer, H. R., & Cannell, D. S. (1983). Universality for static properties of polystyrenes in good and marginal solvents. *Physical Review Letters*, *51*, 1183–1186.

Hamada, F., Kinugasa, S., Hayashi, H., & Nakajima, A. (1984). Small-angle X-ray scattering from semidilute polymer solutions: 1. Polystyrene in toluene. *Macromolecules*, *18*, 2290–2294.

Hardelin, L., Thunberg, J., Perzon, E., Westman, G., Walkenstrom, P., & Gatenholm, P. (2012). Electrospinning of cellulose nanofibers from ionic liquids: The effect of different cosolvents. *Journal of Applied Polymer Science*, *125*, 1901–1909.

Hecht, A.-M., Horkay, F., Schleger, P., & Geissler, E. (2002). Thermal fluctuations in polymer gels investigated by neutron spin echo and dynamic light scattering. *Macromolecules*, *35*, 8552–8555.

Hsu, H.-P., Paul, W., & Binder, K. (2012). Scattering function of semiflexible polymer chains under good solvent conditions. *Journal of Chemical Physics*, *137*, 174902/1–174902/19

Hunt, M. L., Newman, S., Scheraga, H. A., & Flory, P. J. (1956). Dimensions and hydrodynamic properties of cellulose trinitrate molecules in dilute solution. *Journal of Physical Chemistry*, *60*, 1278–1290.

Jia, X., Chen, Y., Shi, Ch., Ye, Y., Wang, P., Zeng, X., et al. (2013). Preparation and characterization of cellulose regenerated from phosphoric acid. *Journal of Agricultural and Food Chemistry*, *61*, 12405–12414.

Johari, N. A., Kudin, T. I. T., Ali, A. M. M., Winie, T., & Yahya, M. Z. A. (2009). Studies on cellulose acetate-based gel polymer electrolytes for proton batteries. *Materials Research Innovations*, *13*, 232–234.

Kamide, K., & Saito, M. (1983). Persistence length of cellulose and cellulose derivatives in solution. *Die Makromolekulare Chemie, Rapid Communications*, *4*, 33–39.

Koddermann, T., Klembt, S., Klasen, D., Paschek, D., Kragl, U., & Ludwig, R. (2012). The effect of neutral ion aggregate formation on the electrical conductivity of an ionic liquid and its mixtures with chloroform. *ChemPhysChem*, *13*, 1748–1752.

Kuzmina, O., Sashina, E., Troshenkowa, S., & Wawro, D. (2010). Dissolved state of cellulose in ionic liquids – the impact of water. *Fibres & Textiles in Eastern Europe*, *18*, 32–37.

Kyllonen, L., Parviainen, A., Deb, S., Lawoko, M., Gorlov, M., Kilpelainen, I., et al. (2013). On the solubility of wood in non-derivatising ionic liquids. *Green Chemistry*, *15*, 2374–2378.

Li, X.-L., Zhu, L.-P., Zhu, B.-K., & Xu, Y.-Y. (2011). High-flux and anti-fouling cellulose nanofiltration membranes prepared via phase inversion with ionic liquid as solvent. *Separation and Purification Technology*, *83*, 66–73.

Luo M., & Neogi A. N. (2009). USA Patent No. 2009/0088564 A1.

Luo, X., & Zhang, L. (2013). New solvents and functional materials prepared from cellulose solutions in alkali/urea aqueous system. *Food Research International*, *52*, 387–400.

Lv, Y., Wu, J., Zhang, J., Niu, Y., Liu, Ch-Y., He, J., et al. (2012). Rheological properties of cellulose/ionic liquid/dimethyl sulfoxide (DMSO) solutions. *Polymer*, *53*, 2524–2531.

McCormick, C. L., Callais, P. A., & Hutchinson, B. H., Jr. (1985). Solution studies of cellulose in lithium chloride and N,N-dimethyl acetamide. *Macromolecules*, *18*, 2394–2401.

Medronho, B., Romano, A., Miguel, M. G., Stigsson, L., & Lindman, B. (2012). Rationalizing cellulose (in)solubility: Reviewing basic physicochemical aspects and role of hydrophobic interactions. *Cellulose*, *19*, 581–587.

Mizumo, T., Marwanta, E., Matsumi, N., & Ohno, H. (2004). Allylimidazolium halides as novel room temperature ionic liquids. *Chemistry Letters*, *33*, 1360–1361.

Pinkert, A., Marsh, K. N., & Pang, Sh. (2010). Reflections on the solubility of cellulose. *Industrial & Engineering Chemistry Research*, *49*, 11121–11130.

Porod, G. (1982). General theory. In O. Glatter, & O. Kratky (Eds.), *Small angle X-ray scattering* (pp. 17–51). London: Academic Press.

Rein, D. M., Khalfin, R., & Cohen, Y. (2012). Cellulose as a novel amphiphilic coating for oil-in-water and water-in-oil dispersions. *Journal of Colloid and Interface Science*, *386*, 456–463.

Remsing, R. C., Liu, Z., Sergeyev, I., & Moyna, G. (2008). Solvation and aggregation of N,N′-dialkylimidazolium ionic liquids: A multinuclear NMR spectroscopy and molecular dynamics simulation study. *Journal of Physical Chemistry B*, *112*, 7363–7369.

Rinaldi, R. (2011). Instantaneous dissolution of cellulose in organic electrolyte solutions. *Chemical Communications*, *47*, 511–513.

Roder, T., & Morgenstern, B. (1999). The influence of activation on the solution state of cellulose dissolved in N-methylmorpholine-N-oxide-monohydrate. *Polymer*, *40*, 4143–4147.

Saalwachter, K., Burchard, W., Klufers, P., Kettenbach, G., Mayer, P., Klemm, D., et al. (2000). Cellulose solutions in water containing metal complexes. *Macromolecules*, *33*, 4094–4107.

Schulz, L., Seger, B., & Buchard, W. (2000). Structures of cellulose in solution. *Macromolecular Chemistry and Physics*, *201*, 2008–2022.

Sescousse, R., Le, K. A., Ries, M. E., & Budtova, T. (2010). Viscosity of cellulose-imidazolium-based ionic liquid solutions. *Journal of Physical Chemistry B*, *114*, 7222–7228.

Song, H., Niu, Y., Wang, Zh., & Zhang, J. (2011). Liquid crystalline phase and gel–sol transitions for concentrated microcrystalline cellulose (MCC)/1-ethyl-3-methylimidazolium acetate (EMIMAc) solutions. *Biomacromolecules*, *12*, 1087–1096.

Stana-Kleinschek, K., & Ribitsch, V. (1998). Electrokinetic properties of processed cellulose fibers. *Colloids and Surfaces A*, *140*, 127–138.

Swatloski, R. P., Spear, S. K., Holbrey, J. D., & Rogers, R. D. (2002). Dissolution of cellulose with ionic liquids. *Journal of the American Chemical Society*, *124*, 4974–4975.

Talmon, Y. (1996). Transmission electron microscopy of complex fluids: The state of the art. *Berichte der Bunsengesellschaft für physikalische Chemie*, *100*, 364–372.

Trap, H. J. L., & Hermans, J. J. (1954). Light-scattering by polymethacrylic acid and carboxymethylcellulose in various solvents. *Journal of Physical Chemistry*, *58*, 757–761.

Vila, J., Gines, P., Pico, J. M., Franjo, C., Jimenez, E., Varela, L. M., et al. (2006). Temperature dependence of the electrical conductivity in EMIM-based ionic liquids: Evidence of Vogel–Tamman–Fulcher behavior. *Fluid Phase Equilibria*, *242*, 141–146.

Vila, J., Gines, P., Rilo, E., Cabeza, O., & Varela, L. M. (2006). Great increase of the electrical conductivity of ionic liquids in aqueous solutions. *Fluid Phase Equilibria*, *247*, 32–39.

Wakai, Ch., Oleinikova, A., Ott, M., & Weingartner, H. (2005). How polar are ionic liquids? Determination of the static dielectric constant of an imidazolium-based

ionic liquid by microwave dielectric spectroscopy. *Journal of Physical Chemistry B*, *109*, 17028–17030.
Wang, H., Gurau, G., & Rogers, R. D. (2012). Ionic liquid processing of cellulose. *Chemical Society Reviews*, *41*, 1519–1537.
Xu, A., Zhang, Y., Zhao, Y., & Wang, J. (2013). Cellulose dissolution at ambient temperature: Role of preferential solvation of cations of ionic liquids by a cosolvent. *Carbohydrate Polymers*, *92*, 540–544.
Zavrel, M., Bross, D., Funke, M., Buchs, J., & Spiess, A. C. (2009). High-throughput screening for ionic liquids dissolving (ligno-)cellulose. *Bioresource Technology*, *100*, 2580–2587.
Zimm, B. H. (1945). Molecular theory of the scattering of light in fluids. *Journal of Chemical Physics*, *13*, 141–145.